Discrete Fracture Model for Hydro-Mechanical Coupling in Fractured Reservoirs

Please fill in the name of the event you are preparing this manuscript for.	The Abu Dhabi International Petroleum Exhibition & Conference (ADIPEC)
Please fill in your 6-digit SPE manuscript number.	SPE-208039-MS
Please fill in your manuscript title.	Discrete Fracture Model for Hydro-Mechanical Coupling in Fractured Reservoirs

Please fill in your author name(s) and company affiliation.

Given Name	Surname	Company
Xupeng	He	King Abdullah University of Science and Technology
Tian	Qiao	King Abdullah University of Science and Technology
Marwa	Alsinan	Saudi Aramco
Hyung	Kwak	Saudi Aramco
Hussein	Hoteit	King Abdullah University of Science and Technology

Abstract

The process of coupled flow and mechanics occurs in various environmental and energy applications, including conventional and unconventional fractured reservoirs. This work establishes a new approach for modeling hydro-mechanical coupling in fractured reservoirs. The discrete-fracture model (DFM), in which the porous matrix and fractures are represented explicitly in the form of unstructured grid, has been widely used to describe fluid flow in fractured formations. In this work, we extend the DFM approach for modeling coupled flow-mechanics process, in which flow problems are solved using the multipoint flux approximation (MPFA) method, and mechanics problems are solved using the multipoint stress approximation (MPSA) method. The coupled flow-mechanics problems share the same computational grid to avoid projection issues and allow for convenient exchange between them. We model the fracture mechanical behavior as a two-surface contact problem. The resulting coupled system of nonlinear equations is solved in a fully-implicit manner. The accuracy and generality of the numerical implementation are accessed using cases with analytical solutions, which shows an excellent match. We then apply the methodology to more complex cases to demonstrate its general applicability. We also investigate the geomechanical influence on fracture permeability change using 2D rock fractures. This work introduces a novel formulation for modeling the coupled flow-mechanics process in fractured reservoirs, and can be readily implemented in reservoir characterization workflow.

Introduction

The process of coupling fluid flow with rock mechanics is found in various environmental and energy applications. Examples include CO_2 sequestration, geothermal energy extraction, water disposal management, and oil & gas recovery in conventional and unconventional fractured reservoirs. Fractured formations are subjected to be more sensitive to the mechanical effects than unfractured ones due to the existence of fractures. This work introduces a new approach for modeling the coupled flow-mechanics process using the DFM for subsurface fractured formations.

For illustration purposes, we divide the coupled flow-mechanics process into two parts: flow problems and mechanics problems. Various conceptual models have been developed to describe flow problems in fractured formations, including dual-porosity and discrete-fracture models. The dual-porosity model has

been widely used for industrial applications due to its simplicity and efficiency. This model dissociates the flow within the porous matrix and fractures and models the matrix-flow interaction via transfer function (also shape factor). Barenblast & Zheltov (1960) first developed the dual-porosity concept and pioneered the study into slightly compressible, single-phase flow problems. Warren & Root (1963) brought the concept to the petroleum industry and assumed the flow occurs only through fractures. Kazemi et al. (1976) extended the Warren & Root model to two-phase flow problems, in which complex physics are considered. Blaskovich et al. (1983) proposed the dual-porosity/dual-permeability model, which allows matrix-matrix flow. These models, however, ignored the spatial variation regarding saturation and pressure within the porous matrix. Later, time- or saturation-dependent transfer functions were introduced by many researchers (e.g., Penuela et al., 2002; Sarma & Aziz, 2006). On the other hand, the DFM is widely considered the most accurate methodology for describing flow behavior in fractured formations and modeling the matrix-fracture interaction. The DFM model represents the porous matrix and fractures explicitly in the form of an unstructured grid and is implemented to model flow behavior herein.

Various numerical techniques based on DFM have been implemented to solve flow problems in fractured media. Within the finite-element (FE) framework, the Galerkin FE method has been applied to simulate single-phase (e.g., Granet et al., 1998; Zhang & Woodbury, 2002) and two-phase flow (e.g., Karimi-Fard & Firoozabadi, 2003; Kim & Deo, 2000). Later, mixed FE method (e.g., Brezzi & Fortin, 2012; Vohralík et al., 2007), discontinuous Galerkin (DG) method (e.g., Cockburn & Shu, 1998), and combined MFE and DG (e.g., Hoteit & Firoozabadi, 2005, 2006, 2008b, 2008a) have received much attention for different physics simulations. Within the finite-volume (FV) framework, two-point flux approximation (TPFA) by Karimi-Fard et al. (2004) and multipoint flux approximation (MPFA) have been introduced (Hajibeygi et al., 2011; Hesse et al., 2008; Matringe et al., 2007; Ţene et al., 2016; Younes et al., 2009). A hybrid approach combining FE and FV has also been explored (Geiger et al., 2004; Matthäi et al., 2007; Monteagudo et al., 2011).

Various numerical attempts have been proposed in the literature to represent mechanics problems. Examples include the Galerkin FE method (Garipov et al., 2014, 2016; Garipov & Hui, 2019), boundary-element method (Crouch et al., 1983), FV multipoint stress approximation (MPSA) method (Keilegavlen et al., 2021; Nordbotten, 2014; Ucar et al., 2018). Subsurface rock fractures exhibit significantly stress-dependent, nonlinear mechanical behavior. Herein, we model the mechanical behavior of the fractures as a contact problem between two surfaces. A mechanical model for the fractures needs to characterize the changes in the stress (including normal and shear stresses) and the displacement (including normal and tangential components) fields. A review of almost all models used to quantify the relation between hydraulic properties of rock fractures and (effective) normal stress is summarized by (X. He et al., 2020). Complex variations in fracture geometry occur during shearing, making it challenging to characterize fracture stress-dependent hydraulic behaviors theoretically. Still, many experimental efforts have been put in the literature (Javadi et al., 2014; Wang et al., 2020; Watanabe et al., 2009). However, limited theoretical or empirical models have been proposed in the literature to account for the relation between fracture permeability and shear stress.

In this work, we incorporate the coupling flow-mechanics process into the DFM. The flow problems in the porous rock (porous matrix and fractures) are solved using the MPFA method, while the mechanics are solved using the MPSA method. Both solver moduli have been implemented within the MRST framework (A. Lie, 2019). The coupled flow-mechanics problems share the same computational grid, which allows for convenient information exchange between them and also avoids projection issues. We model the mechanical behavior of fractures as a nonlinear contact problem between two computational planes. The resulting coupled system of nonlinear equations is solved in a fully-implicit manner. We validate the proposed numerical formulation on simple cases with analytical solutions. General applicability is demonstrated for more complex cases. We also investigate the geomechanical influence

on fracture permeability change using 2D rock fractures. This work introduces a novel formulation for modeling the coupled flow-mechanics process based on DFM in subsurface fractured reservoirs. It can be readily used to represent main faults/fractures at large-scale and upscale effective properties for a representative volume of fractured rock at small-scale.

Governing Equations

In this section, we present the governing equations for describing coupled flow and mechanics behaviors in fully-saturated porous rock with fractures. We separate the porous rock into porous matrix and fractures for modeling purposes. Herein, we assume a compressible, single-phase fluid in an isothermal system.

1. Porous Matrix

Flow Equation: Combining Darcy's law and mass conservation equation yields the flow equation for modeling flow behavior:

$$\frac{\partial\left(\rho_f \phi\right)}{\partial t} = \nabla\cdot\left[\frac{\rho_f k}{\mu_f}\left(\nabla p - \rho_f \vec{g}\right)\right] + q \tag{1}$$

Where ρ_f and μ_f are the density and viscosity of the fluid, respectively; ϕ and k are the porosity and permeability of the porous matrix, respectively; p is the fluid pressure; $\vec{g}$ is the gravity vector; q is the source term.

Mechanics Equation: The mechanics equation for fully-saturated porous matrix (pore fluid + solid skeleton) is described by the quasi-static Cauchy equation:

$$\nabla\cdot\vec{\vec{\sigma}} + \rho\vec{g} = 0 \tag{2}$$

Where $\vec{\vec{\sigma}}$ is the total stress tensor, honoring the contributions from both pore fluid and solid skeleton; ρ is the overall density with $\rho = \rho_s\left(1-\phi\right) + \rho_f\phi$. In this equation, ρ_s is the solid density. The relation between total stress and effective stress tensors is expressed as:

$$\vec{\vec{\sigma}} = \vec{\vec{\sigma}}' + b\vec{\vec{I}}p \tag{3}$$

Where $\vec{\vec{\sigma}}'$ is the effective stress tensor, b is the Biot parameter, $\vec{\vec{I}}$ is the second-order unit tensor, p is the fluid pressure. We assume a linear relationship between the stress and strain tensors, such that:

$$\vec{\vec{\sigma}}' = \vec{\vec{C}} : \vec{\vec{\varepsilon}} \tag{4}$$

Where $\vec{\vec{C}}$ is the fourth-order linear elastic stiffness tensor; $\vec{\vec{\varepsilon}}$ is the strain tensor expressed as a function of the displacement vector $\vec{u}$ and takes the form $\vec{\vec{\varepsilon}} = \frac{1}{2}\left(\nabla\vec{u} + \nabla^T\vec{u}\right)$.

The porosity of the porous matrix is sensitive to changes in the stress and strain fields. The porosity dependence has the form (Coussy, 2004):

$$\phi = \phi_{ref} + \frac{\left(b-\phi_{ref}\right)\left(1-b\right)}{K_d}\left(p - p_{ref}\right) + b\left(\varepsilon_v - \varepsilon_{v,ref}\right) \tag{5}$$

Where ϕ_{ref} , p_{ref} , and $\varepsilon_{v,ref}$ are the reference porosity, pressure, and volumetric strain, respectively. The volumetric strain ε_v is defined as $\varepsilon_v = \sum_i \varepsilon_{ii}$, and K_d is the drained bulk modulus. In this study, the changes in permeability of porous matrix are assumed to be negligible.

2. Fractures

Flow Equation: Eq. (1) is used to describe flow in fractures under the assumption of a laminar flow regime. We assume the fracture porosity to be constant yet with strongly stress-dependent permeability.

Mechanics Equation: Natural rock fractures are formed of two surfaces with anisotropic roughness, varying aperture, and contact areas. Subsurface rock fractures exhibit significantly stress-dependent, nonlinear mechanical behavior. Herein, we model the fracture mechanical behavior as a two-surface contact problem. A mechanical model for the fractures is required to characterize the relation between the stress (including normal and shear stresses) and the displacement (including normal and shear components) fields. **Figure 1** illustrates a fracture modeled as two rough surfaces in contact (a) and its parallel representation with certain reference width (b). The reference width (denoted as g_{ref}) is defined based on the surface roughness. We define normal displacement (denoted as g_N) as the distance relative to the reference width g_{ref} and shear displacement (denoted as g_T) as the distance of the displacement vector in the direction of the fracture. We summarize three statuses (compression, stress-free, and dilation) and corresponding values into Eq. (6).

$$g_N \begin{cases} > 0 & compression \\ = 0 & stress - free \\ < 0 & dilation \end{cases} \tag{6}$$

The stress $\vec{t}$, acting on the fracture surface, could be represented by two parts, as shown in **Figure 1**, which has the form:

$$\vec{t} = t_N \vec{n} + t_T \vec{\tau} \tag{7}$$

Where t_N and t_T are normal and shear stresses acting on the fracture surfaces, respectively.

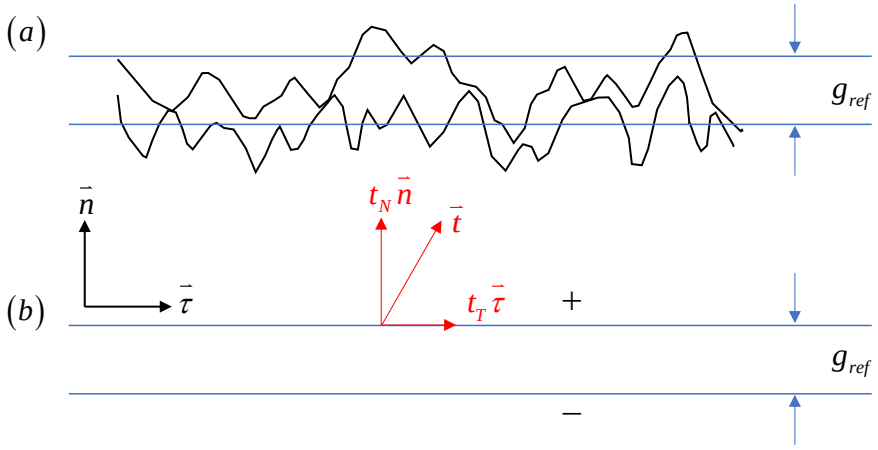

Figure 1. Fractures represented by rough surfaces with contacts (a) and its parallel representation with

a certain reference width (b).

The acting stresses are assigned to each of the fracture surfaces using symbols "+" and "-", as shown in **Figure 1**. Imposing the continuity conditions yields:

$$\begin{aligned} t_N &= t_N^+ = -t_N^- \\ t_T &= t_T^+ = -t_T^- \end{aligned} \tag{8}$$

The mechanical model for the fractures characterizes the relation between acting stress and corresponding displacements (including normal and tangential components), which is described as:

$$\begin{aligned} t_N &= \square\left(g_N\right) \\ t_T &= F\left(t_N\right) \quad for \quad g_T \neq 0 \quad \left(slip\right) \\ t_T &< F\left(t_N\right) \quad for \quad g_T = 0 \quad \left(stick\right) \end{aligned} \tag{9}$$

Where $\square$ represents the relation between (effective) normal stress, denoted as t_N, and normal displacement g_N. F represents the friction law. **Figure 2**, left, shows a typical relation between normal stress and its corresponding displacements. The behaviors during shearing are complex and are dependent on both normal and shear stresses. The shearing could be characterized using two states: "slip" or "stick". The fracture is in a "stick" state under the condition of shear stress (denoted as t_T) below the envelope curve (blue line in **Figure 2**). "Slip" state occurs when t_T reaches the envelope curve, and corresponding shear displacement is calculated by the second equation in Eq. (9).

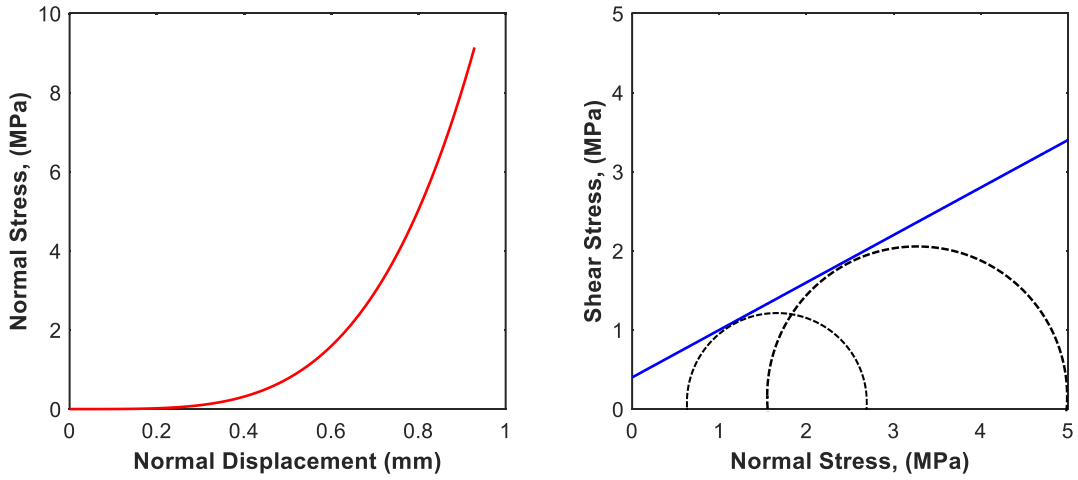

Figure 2. Normal stress versus normal displacement (left) and the friction law defining the relation between shear stress and normal stress.

The fracture hydraulic conductivity, denoted by C_f, is given by the following expression (Garipov et al., 2016; Garipov & Hui, 2019):

$$C_f = -\frac{g_N^3}{12} + C_{f,ref} \tag{10}$$

We note that Eq. (10) is valid for $g_N \geq 0$, which corresponds to the compression or stress-free status. For negative normal displacement, representing dilation status, the two surfaces lose physical contact, and its hydraulic conductivity are given by cubic-law-based models. A comprehensive review of various cubic-law-based models has been studied by (Xupeng He et al., 2021).

Validation: Numerical Implementation

In this section, we demonstrate the accuracy and superiority of numerical implementation using three cases that have analytical solutions. In this first case, we validate the accuracy and generality of the MPFA method with the linear flow problem without fractures. In the second case, we validate the MPFA-MPSA implementation with Mandel problem in porous matrix without fractures. Finally, we validate the MPSA implementation with Sneddon problem with fracture deformation. The three cases correspond to flow-only, coupled flow-mechanics, mechanic-only problems.

1) Linear Flow Problem

We first validate the accuracy and generality of MPFA method by considering a 2D linear flow problem. **Figure 3** depicts the problem domain (left) and its implemented computational grid (right). We define the domain with the dimension of $10m \times 10m$, and assume the permeability to be homogeneous and isotropic. We consider an incompressible, single-phase flow problem with pressure difference imposed on two opposite boundaries and no-flux on the other two boundaries (**Figure 3**, left). This problem exhibits a simple analytical solution, given by $p(x) = 10 - x$.

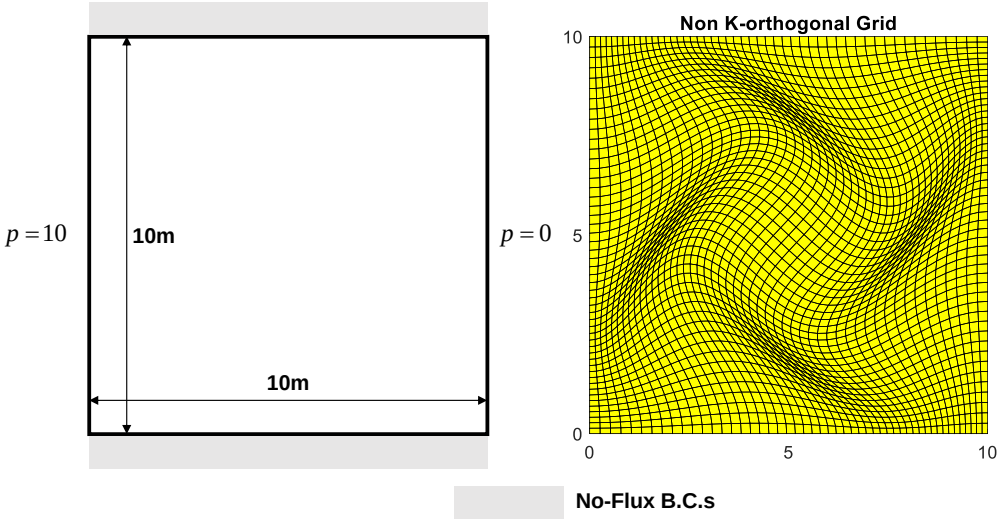

Figure 3. Simulation domain with boundary conditions (left), and the unstructured computational grid (right).

The standard two-point flux approximation (TPFA) method is widely used as the industry standard for discretizing flow equations due to its simplicity and efficiency. The method is known to introduce numerical errors and poor convergence when the grid deviates from the K-orthogonal property. Guaranteeing K-orthogonality is a difficult problem when representing complex geological features, including fractures, faults, among others. The MPFA method addresses the issue by approximating the inter-cell face flux using more than two points, and therefore could be applicable for grids that are not necessarily K-orthogonal. A detailed implementation of MPFA method could be found in the references (Aavatsmark, 2002; K. A. Lie et al., 2012).

The implemented computation grid is a skewed, curvilinear grid with most grid cells are not K-orthogonal (**Figure 3**, right). We compare the MPFA pressure solution with solutions computed by the analytical and TPFA methods. **Figure 4** shows the pressure field computed by three different methods: analytical (left), MPFA (middle), and TPFA (right) with the same setup in **Figure 3**. The MPFA pressure solution shows an excellent match with analytical solutions, while the TPFA solution shows significant errors caused by the grid-orientation effect, as expected. The MPFA scheme honors the consistency and convergence on the grid that is not K-orthogonal, which shows general applicability for other complex cases.

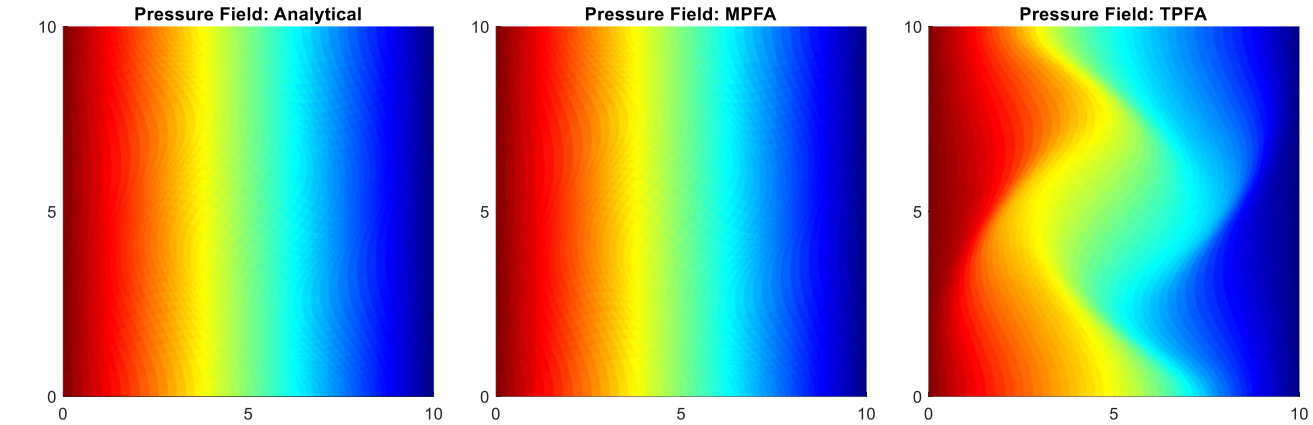

Figure 4. Pressure field solutions by three different methods: analytical (left), MPFA (middle), and TPFA (right).

2) Mandel Problem

In this case, we consider the 2D Mandel consolidation problem (Mandel, 1953), which has an analytical solution. Mandel problem is commonly used to validate the accuracy and generality of numerical implementation for problems with coupled flow and mechanics. Herein, the coupled MPFA-MPSA scheme is verified. The Mandel problem describes an isotropic poroelastic slab sandwiched by two rigid plates (see **Figure 5**, left). Initially, the top and bottom slabs are assigned by a constant compressive force, respectively. The force intensity is $2F$. Gravity effect is neglected in this study. We perform computations on a quarter domain, denoted by Ω, instead of the full domain due to the symmetry of the problem. The imposed boundary conditions on the quarter domain are shown in **Figure 5**, right.

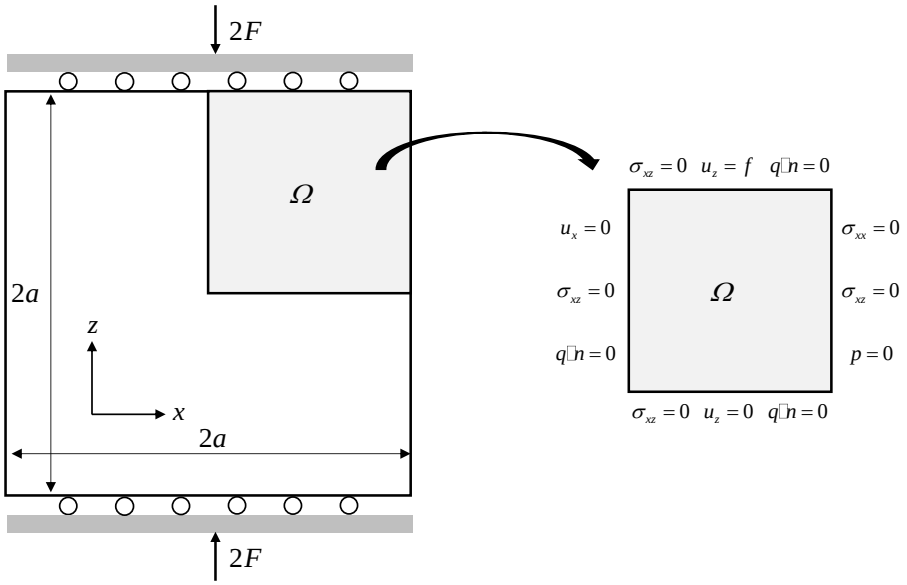

Figure 5. Mandel problem with a square domain, where the geometric setup is shown on the left, and positive quarter domain with imposed boundary conditions on the right.

The coupled flow-mechanics problem is modeled using the equations in the "porous matrix" subsection with MPFA for flow and MPSA for mechanics. We ensure numerical stability by increasing the number of grid cells until the two consecutive solutions are within 0.1 %. The implemented computation grid is structured with 100×50 square cells. The simulation parameters used are as follows: Young modulus $1.5\times10^4 MPa$, Biot modulus 1, Poisson ratio 0.2, porosity 0.2, fluid viscosity $2cP$, and permeability $1000mD$. In our calculations, we assume the fluid to be incompressible. **Figure 6** illustrates the comparison between analytical (dots) and coupled MPFA-MPSA solutions in terms of normalized pressure, which shows an excellent match. Although Mandel problem does not contain the fractures, its successful implementation of proposed MPFA-MPSA schemes shows great potential for modeling hydro-mechanical coupling process in fractured reservoirs. Its generality in fractured formations is demonstrated in the next section.

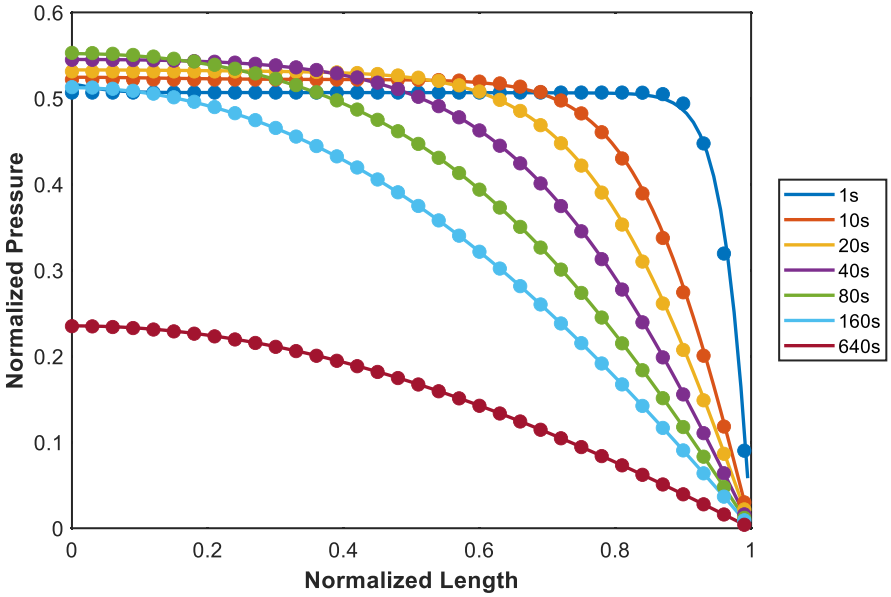

Figure 6. Normalized pressure versus normalized length solved by analytical (dots) and coupled MPFA-MPSA (solid lines) methods.

3) Sneddon Problem

In this case, we validate the MPSA implementation for fracture deformation with Sneddon problem (mechanics-only problem). We consider a 2D square domain of porous rock with a single fracture located at the center. The fracture aligns with the horizontal direction and is subjected to a constant pressure p acting on each side of the fracture (see **Figure 7**, left). For an infinite elastic domain, Sneddon (1995) provided an analytical solution for the relative normal displacement $[\![u_j]\!]_n$ along the fracture:

$$[\![u_j]\!]_n = \frac{(1-\upsilon)\,pL}{G}\sqrt{1-\frac{d_f^2}{(L/2)^2}} \tag{11}$$

Where G and υ are shear modulus and Poisson's ratio, respectively; L is fracture length; d_f is the distance from the fracture center.

The related parameters used herein are collected from the reference (Tao, 2010) with $G = 9.06 \times 10^5\ psi$, $\upsilon = 0.2$, $L = 39.37 inch$ and $p = 145 psi$. In our MPSA simulation, we mimic the condition of an infinite domain using a Dirichlet boundary, in which we set the prescribed displacement to be equal to the analytical solution computed following the procedure in the reference (Crouch et al., 1983). We ensure numerical stability by increasing the number of grid cells until the two consecutive solutions are within 0.1 %. **Figure 7**, right, shows the comparison in terms of relative normal displacement solved by analytical and MPSA methods, and the results show an excellent match. We demonstrate the accuracy of the MPSA method using the Sneddon problem. A detailed implementation of the MPSA method could be found in the references (Keilegavlen et al., 2021; Nordbotten, 2014; Ucar et al., 2018).

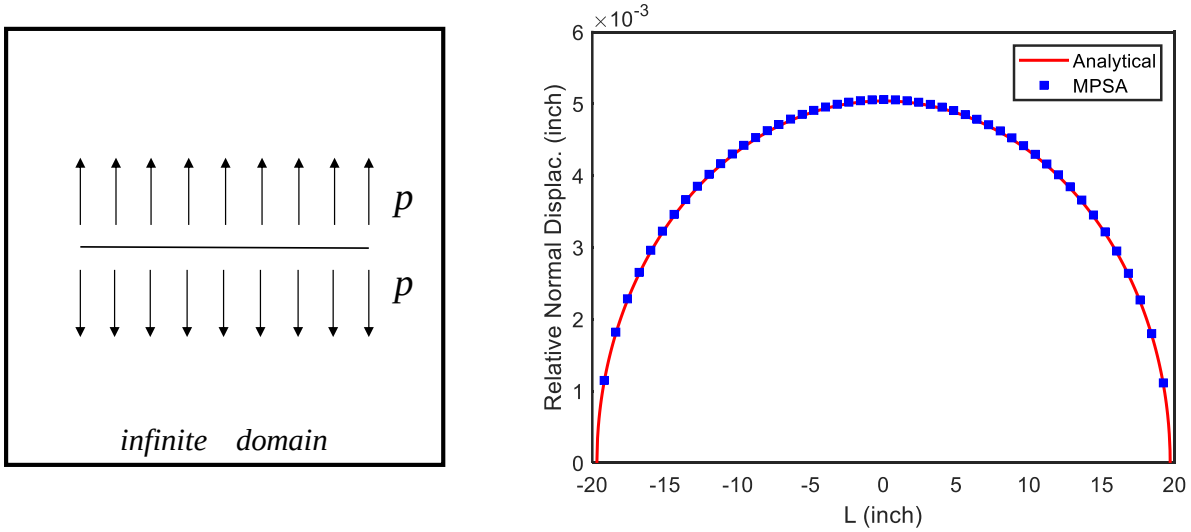

Figure 7. Sneddon problem setup (left), and comparison between analytical and MPSA methods (right).

Application: Coupled Flow-Mechanics

General applicability is demonstrated in this section by applying the proposed methodology to a more complex case. In addition, geomechanical influence on single rock fracture is investigated. We solve the coupled-mechanics problems based on discrete-fracture representation, which incorporates all the elements mentioned above. We consider a subsurface domain bounded by $(-50,50)\times(-800,-700)m^2$.

Figure 8 (a) shows the problem domain with four non-intersecting fractures, in which the fracture highlighted in red, denoted by Facture I, includes an injector. Gravity is taken into consideration. We set a 20-day injection period and an anisotropic stress regime. Boundary and initial conditions are defined as follow:

B.C.s: Hydrostatic and lithostatic boundary conditions are applied at all edges:

$$\begin{aligned} p &= p_{atm} - \rho_f g z \\ \sigma \cdot n - \alpha p n &= \rho_s g c_{ani} n \end{aligned} \tag{12}$$

Where p_{atm} is atmospheric pressure and c_{ani} is anisotropy ratio for x and z directions. Other parameters are defined in the previous section.

I.C.s: Initially, the system is at the equilibration state:

$$p_{ini} = p_{atm} - \rho_f g z$$
$$\left(g_N^{ini}, g_T^{ini}\right) = (0,0)\, m \tag{13}$$

The other simulation parameters are collected from the example case from subsection 6.2 (Keilegavlen et al., 2021). The porous matrix is discretized using triangle cells, and fractures are characterized using 1D lines. The resulting nonlinear equations are discretized by MPFA-MPSA with temporal discretization in an implicit Euler formulation. Numerical stability is ensured by increasing the grid elements until the two consecutive solutions are within 0.1 %. **Figure 8** (b) summarizes fracture dynamics during the injection period, which highlights the necessity and superiority of explicit fracture representation in capturing complicated fracture deformation.

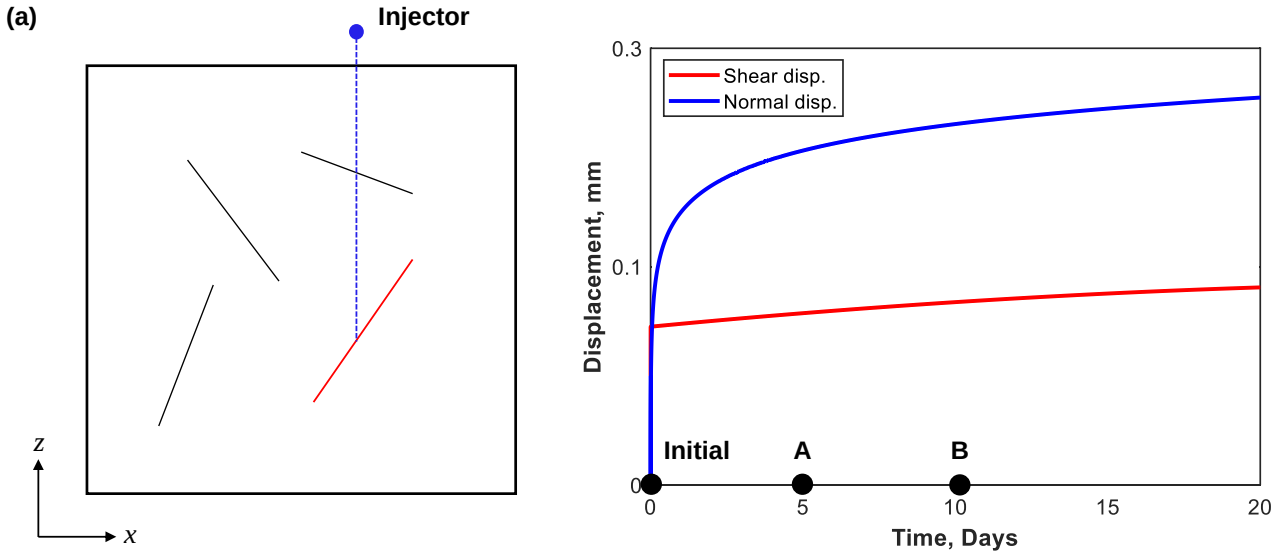

Figure 8. Problem domain with fractures and a well (a) and Normal & shear displacements for Fracture I (b).

We then investigate the geomechanical effect on fracture permeability change using Fracture I. The geomechanical effect investigated herein including pure normal, pure shear, and combined stresses. The initial effective hydraulic permeability of Fracture I is computed by a given 2D rock fracture under stress-free conditions (denoted as "initial"), as shown in **Figure 9**. Fracture profiles under different stress states could be obtained based on displacement curves in **Figure 8**. Herein, we mimic the normal or shear process by shifting the top surface in the normal or tangential direction yet fixing the bottom surface. We summarize the corresponding fractures under different displacement conditions in **Figure 9**. g_N^A represents normal displacement in state **A** with positive values for compression while negative ones for dilation. g_T^A represents shear displacement in state **A** with positive values for x-positive-direction shifting while negative values for x-negative-direction shifting.

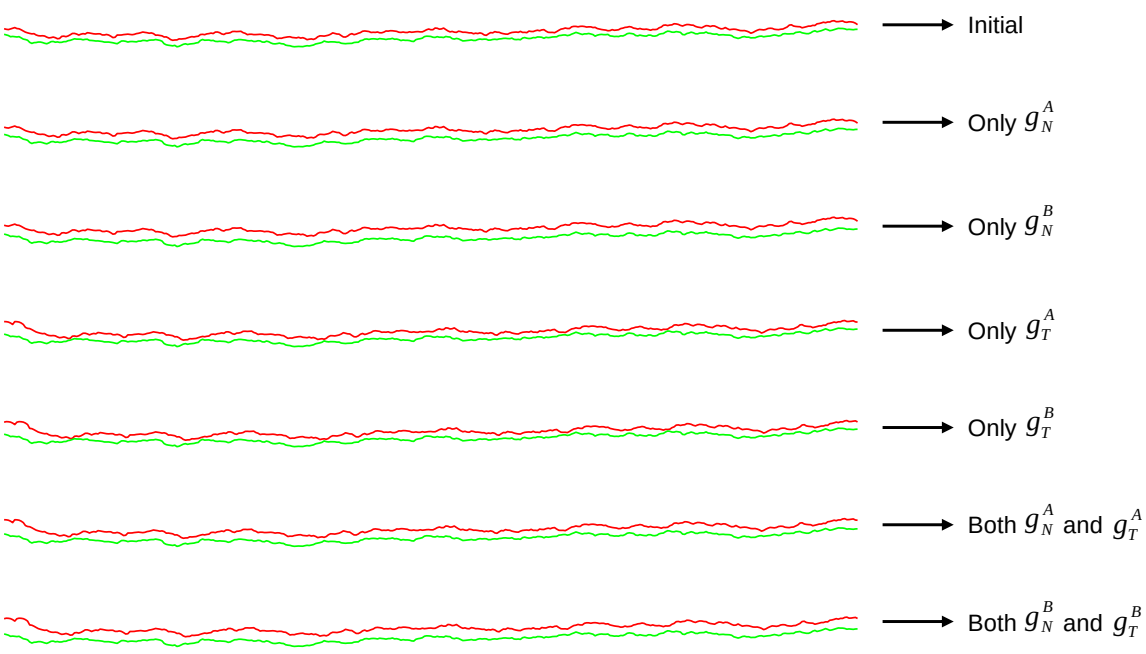

Figure 9. Fracture profiles under different stress conditions: “initial”, “A”, and “B”.

The effective hydraulic permeabilities for resulting new fractures are computed by applying high-resolution Navier-Stokes (NS) equations. Fluid flow inside fractures is assumed to be laminar. A detailed description of the numerical implementation of NS equations is proved in **Appendix A**. Numerical stability is ensured by increasing the number of grid elements until the consecutive two solutions are within 0.1 %. Permeability change versus stress status is summarized in **Figure 10**. We observe in **Figure 10** the fracture permeability increases significantly from state initial to state **B** for both only normal and combined cases. As the fluid is injected into the fracture, the dilation process occurs with increasing pressure. Meanwhile, shearing process may invoke when shear stress exceeds the envelop curve. In our case, shearing decreases the fracture permeability by introducing a mismatch between the two surfaces. We demonstrate the geomechanical effects on fracture permeability based on 2D rock fractures. The coupled hydro-mechanical process should be highly paid attention to, especially in naturally fractured reservoirs. More realistic 3D cases will be focused on in future work.

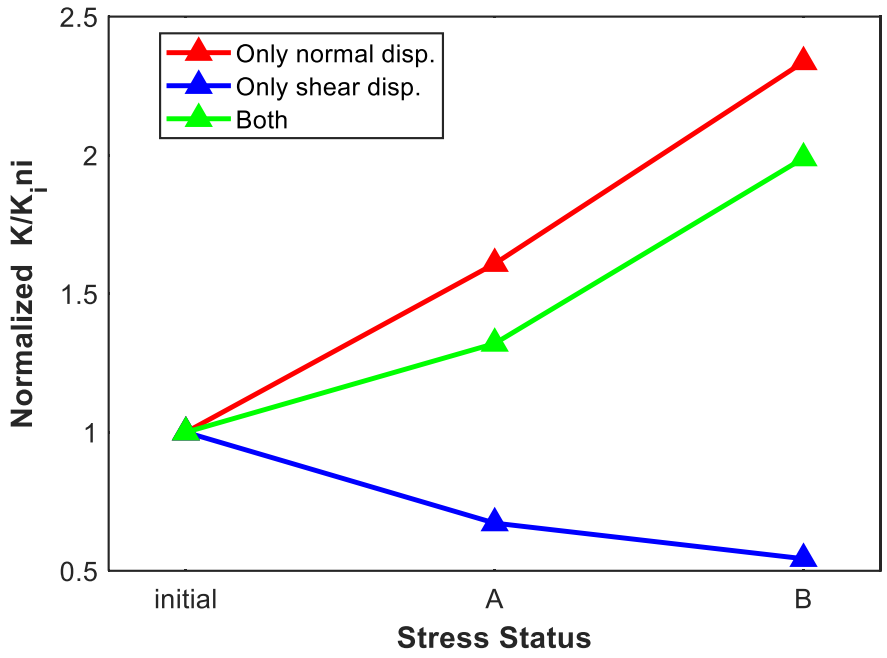

Figure 10. Normalized permeability versus stress under different schemes.

Conclusions

We extended the discrete-fracture model for modeling coupled flow and mechanics processes in fractured reservoirs. We proposed a novel numerical approach combining the MPFA for flow problems and MPSA for mechanical problems. The two numerical methods share the same computational grid, which accelerates the information exchange between the coupled flow and mechanics problems and avoids the projection issue. Our proposed numerical implementation incorporates the mechanical behavior of fractures as a nonlinear contact problem between two fracture surfaces. The resulting coupled system of nonlinear equations is solved in a fully-implicit manner. The associated implementation is developed within the MRST platform, which allows for more comprehensive physics like multi-phase and multi-component, and more general applications such as simulating coupled thermo-hydro-mechanical effects in fractured geothermal reservoirs.

We demonstrate the accuracy of the numerical formulation with three problems with analytical solutions. General applicability is demonstrated for a more complex case with fracture networks. The geomechanical effects on fracture permeability change are also investigated based on 2D rock fractures. This work introduces a novel formulation for modeling the coupled flow-mechanics process based on DFM in subsurface fractured reservoirs. It can be readily used to represent main faults/fractures at large-scale and upscale effective properties for a representative volume of fractured rock at a small-scale. Future work could focus on incorporating localized effects of fracture roughness and 3D subsurface fractured formations.

Acknowledgments

We would like to thank Saudi Aramco for funding this research. We would also like to thank King Abdullah University of Science and Technology (KAUST) for providing a license of MATLAB.

Additional Information

Discussion is highly encouraged regarding any question about this paper. All simulation codes are available upon request. All codes are developed in MATLAB within the MRST framework. Citing this paper is needed when implementing the codes developed by the authors.

Appendix A: Mixed Finite Element Formulation for NS Equations

Consider the steady-state of incompressible, Newtonian flow with no gravity effects, and the full-physics NS equations can be given as:

$$\begin{aligned} \rho\left(\vec{u}\bullet\nabla\vec{u}\right) &= -\nabla p+\mu\nabla^2\vec{u} \\ \nabla\bullet\vec{u} &= 0 \end{aligned} \tag{A1}$$

In the above equations, ρ is fluid density, $\vec{u}$ is velocity vector, p is pressure, and μ is fluid viscosity. No-slip boundary conditions are assigned to the fracture walls, and pressure values are imposed at the inlet and outlet of fracture (see **Figure A1**). The gradient of velocity in the direction of pressure gradient is set to zero to guarantee the fully developed flow and to avoid the inlet effect.

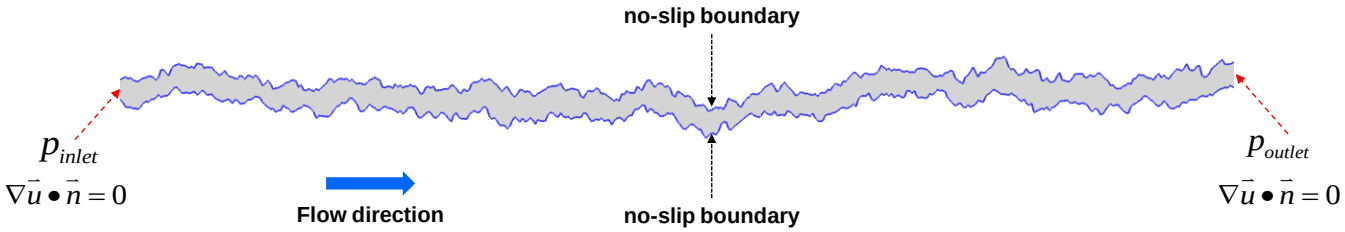

Figure A1. Illustration of boundary conditions imposed on a rough-walled fracture.

The NS equations can be formulated in a mixed variational form, where the velocity, and the pressure, are approximated simultaneously. Multiplying Eq. (A1) by the test function $\left(\vec{v},q\right)$ and integrating the resulting equations over the domain Ω yields:

$$\begin{aligned} \int_\Omega \rho\left(\vec{u}\bullet\nabla\vec{u}\right)\bullet\vec{v}dx &= \int_\Omega\left(-\nabla p\right)\bullet\vec{v}dx+\int_\Omega\left(\mu\nabla^2\vec{u}\right)\bullet\vec{v}dx \\ \int_\Omega\left(\nabla\bullet\vec{u}\right)qdx &= 0 \end{aligned} \tag{A2}$$

Applying the integration by parts technique, we have:

$$\begin{aligned} \int_\Omega\left(-\nabla p\right)\bullet\vec{v}dx &= \int_\Omega p\nabla\bullet\vec{v}dx-\int_{\partial\Omega}p\vec{v}\bullet\vec{n}ds \\ \int_\Omega\left(\mu\nabla^2\vec{u}\right)\bullet\vec{v}dx &= -\mu\int_\Omega\nabla\vec{u}:\nabla\vec{v}dx+\mu\int_{\partial\Omega}\nabla\vec{u}\bullet\vec{n}\vec{v}ds \end{aligned} \tag{A3}$$

Using the abstract framework, we have the problem find $\left(\vec{u},p\right)\in W$ such that

$$a\left(\left(\vec{u},p\right),\left(\vec{v},q\right)\right)=L\left(\left(\vec{v},q\right)\right) \tag{A4}$$

For all $\left(\vec{v},q\right)\in W$, where

$$a\left(\left(\vec{u},p\right),\left(\vec{v},q\right)\right)=\rho\int_{\Omega}\left(\vec{u}\bullet\nabla\vec{u}\right)\bullet\vec{v}dx-\int_{\Omega}p\nabla\bullet\vec{v}dx+\mu\int_{\Omega}\nabla\vec{u}:\nabla\vec{v}dx+\int_{\Omega}\left(\nabla\bullet\vec{u}\right)qdx \tag{A5}$$

$$L\left(\left(\vec{v},q\right)\right)=-\int_{\partial\Omega_N}p_{inlet}\vec{v}\bullet\vec{n}ds-\int_{\partial\Omega_N}p_{outlet}\vec{v}\bullet\vec{n}ds \tag{A6}$$

The space W should be a mixed-function space: $W=V\times Q$ such that $\vec{u}\in V$ and $q\in Q$.

References

Aavatsmark, I. (2002). An introduction to multipoint flux approximations for quadrilateral grids. *Computational Geosciences*, *6*(3–4), 405–432. https://doi.org/10.1023/A:1021291114475

Barenblast, G. I., & Zheltov, Y. P. (1960). Fundamental equations of filtration of homogeneous liquids in fissured rocks. *Soviet Physics Doklady*.

Blaskovich, F. T., Cain, G. M., Sonier Fernand, Waldren, D., & Webb, S. J. (1983). Multicomponent Isothermal System for Efficient Reservoir Simulation. *Society of Petroleum Engineers of AIME, (Paper) SPE*, 305–322. https://doi.org/10.2523/11480-ms

Brezzi, F., & Fortin, M. (2012). *Mixed and hybrid finite element methods* (Vol. 15). Springer Science & Business Media.

Cockburn, B., & Shu, C. W. (1998). The Runge–Kutta Discontinuous Galerkin Method for Conservation Laws V. *Journal of Computational Physics*, *141*(2), 199–224.

Crouch, S. L., Starfield, A. M., & Rizzo, F. J. (1983). *Boundary element methods in solid mechanics*.

Garipov, T. T., & Hui, M. H. (2019). Discrete Fracture Modeling approach for simulating coupled thermo-hydro-mechanical effects in fractured reservoirs. *International Journal of Rock Mechanics and Mining Sciences*, *122*(November 2018), 104075. https://doi.org/10.1016/j.ijrmms.2019.104075

Garipov, T. T., Karimi-Fard, M., & Tchelepi, H. A. (2014). Fully coupled flow and geomechanics model for fractured porous media. *48th US Rock Mechanics / Geomechanics Symposium 2014*, *2*, 1174–1182.

Garipov, T. T., Karimi-Fard, M., & Tchelepi, H. A. (2016). Discrete fracture model for coupled flow and geomechanics. *Computational Geosciences*, *20*(1), 149–160. https://doi.org/10.1007/s10596-015-9554-z

Geiger, S., Roberts, S., Matthäi, S. K., Zoppou, C., & Burri, A. (2004). Combining finite element and finite volume methods for efficient multiphase flow simulations in highly heterogeneous and structurally complex geologic media. *Geofluids*, *4*(4), 284–299. https://doi.org/10.1111/j.1468-8123.2004.00093.x

Granet, S., P, F., P, L., & M, Q. (1998). A single phase flow simulation of fractured reservoir using a discrete representation of fractures.

Hajibeygi, H., Karvounis, D., & Jenny, P. (2011). A hierarchical fracture model for the iterative multiscale finite volume method. *Journal of Computational Physics*, *230*(24), 8729–8743. https://doi.org/10.1016/j.jcp.2011.08.021

He, X., Hoteit, H., AlSinan, M. M., & Kwak, H. T. (2020). Modeling hydraulic response of rock fractures under effective normal stress. *ARMA/DGS/SEG International Geomechanics Symposium 2020, IGS 2020*.

He, Xupeng, Sinan, M., Kwak, H., & Hoteit, H. (2021). A corrected cubic law for single-phase laminar flow through rough-walled fractures. *Advances in Water Resources*, *154*, 103984. https://doi.org/10.1016/J.ADVWATRES.2021.103984

Hesse, M. A., Mallison, B. T., & Tchelepi, H. A. (2008). Compact multiscale finite volume method for heterogeneous anisotropic elliptic equations. *Multiscale Modeling and Simulation*, *7*(2), 934–962. https://doi.org/10.1137/070705015

Hoteit, H., & Firoozabadi, A. (2005). Multicomponent fluid flow by discontinuous Galerkin and mixed

methods in unfractured and fractured media. *Water Resources Research*, *41*(11), 1–15. https://doi.org/10.1029/2005WR004339

Hoteit, Hussein, & Firoozabadi, A. (2006). Compositional modeling of discrete-fractured media without transfer functions by the discontinuous Galerkin and mixed methods. *SPE Journal*, *11*(3), 341–352. https://doi.org/10.2118/90277-PA

Hoteit, Hussein, & Firoozabadi, A. (2008a). An efficient numerical model for incompressible two-phase flow in fractured media. *Advances in Water Resources*, *31*(6), 891–905. https://doi.org/10.1016/j.advwatres.2008.02.004

Hoteit, Hussein, & Firoozabadi, A. (2008b). Numerical modeling of two-phase flow in heterogeneous permeable media with different capillarity pressures. *Advances in Water Resources*, *31*(1), 56–73. https://doi.org/10.1016/j.advwatres.2007.06.006

Javadi, M., Sharifzadeh, M., Shahriar, K., & Mitani, Y. (2014). Critical Reynolds number for nonlinear flow through rough-walled fractures: The role of shear processes. *Water Resources Research*, *50*(2), 1789–1804.

Karimi-Fard, M., & Firoozabadi, A. (2003). Numerical Simulation of Water Injection in Fractured Media Using the Discrete Fractured Model and the Galerkin Method. *SPE Reserv. Eval. Eng.*, *6*(2), 117–126.

Karimi-Fard, Mohammad, Durlofsky, L. J., & Aziz, K. (2004). An efficient discrete-fracture model applicable for general-purpose reservoir simulators. *SPE Journal*, *9*(2), 227–236. https://doi.org/10.2118/88812-PA

Kazemi, H., Merrill, L. S., Porterfield, K. L., & Zeman, P. R. (1976). Numerical Simulation of Water-Oil Flow in Naturally Fractured Reservoirs. *Soc Pet Eng AIME J*, *16*(6), 317–326. https://doi.org/10.2118/5719-pa

Keilegavlen, E., Berge, R., Fumagalli, A., Starnoni, M., Stefansson, I., Varela, J., & Berre, I. (2021). PorePy: an open-source software for simulation of multiphysics processes in fractured porous media. *Computational Geosciences*, *25*(1), 243–265. https://doi.org/10.1007/s10596-020-10002-5

Kim, J. G., & Deo, M. D. (2000). Finite element, discrete-fracture model for multiphase flow in porous media. *AIChE Journal*, *46*(6), 1120–1130. https://doi.org/10.1002/aic.690460604

Lie, A. (2019). *An Introduction to Reservoir Simulation Using MATLAB/GNU Octave*. Cambridge University Press. https://doi.org/10.1017/9781108591416

Lie, K. A., Krogstad, S., Ligaarden, I. S., Natvig, J. R., Nilsen, H. M., & Skaflestad, B. (2012). Open-source MATLAB implementation of consistent discretisations on complex grids. *Computational Geosciences*, *16*(2), 297–322. https://doi.org/10.1007/s10596-011-9244-4

Matringe, S. F., Juanes, R., & Tchelepi, H. A. (2007). Mixed finite element and related control volume discretizations for reservoir simulation on three-dimensional unstructured grids. *SPE Reservoir Simulation Symposium Proceedings*, *Di*(2), 201–213. https://doi.org/10.2118/106117-ms

Matthäi, S. K., Mezentsev, A., & Belayneh, M. (2007). Finite element-node-centered finite-volume two-phase-flow experiments with fractured rock represented by unstructured hybrid-element meshes. *SPE Reservoir Evaluation and Engineering*, *10*(6), 740–756. https://doi.org/10.2118/93341-pa

Monteagudo, J. E. P., Rodriguez, A. A., & Florez, H. (2011). Simulation of flow in discrete deformable fractured porous media. *Society of Petroleum Engineers - SPE Reservoir Simulation Symposium 2011*, *1*(February), 276–291.

Nordbotten, J. M. (2014). Finite volume hydromechanical simulation in porous media. *Water Resources Research*, *50*(5), 4379–4394. https://doi.org/10.1002/2013WR014979.Reply

Penuela, G., Civan, F., Hughes, R. G., & Wiggins, M. L. (2002). Time-Dependent Shape Factors for Interporosity Flow in Naturally Fractured Gas-Condensate Reservoirs. *SPE Proceedings - Gas Technology Symposium*, 183–200. https://doi.org/10.2118/75524-ms

Sarma, P., & Aziz, K. (2006). New transfer functions for simulation of naturally fractured reservoirs with dual-porosity models. *SPE Journal*, *11*(3), 328–340. https://doi.org/10.2118/90231-PA

Sneddon, I. N. (1995). *Fourier transforms*. *Courier Corporation*.

Tao, Q. (2010). *Numerical Modeling of Fracture Permeability Change in Naturally Fractured Reservoirs Using a Fully Coupled Displacement Discontinuity Method*. Texas A&M University.

Ţene, M., Al Kobaisi, M. S., & Hajibeygi, H. (2016). Algebraic multiscale method for flow in heterogeneous porous media with embedded discrete fractures (F-AMS). *Journal of Computational Physics*, *321*, 819–845. https://doi.org/10.1016/j.jcp.2016.06.012

Ucar, E., Berre, I., & Keilegavlen, E. (2018). Three-Dimensional Numerical Modeling of Shear Stimulation of Fractured Reservoirs. *Journal of Geophysical Research: Solid Earth*, *123*(5), 3891–3908. https://doi.org/10.1029/2017JB015241

Vohralík, M., Maryška, J., & Severýn, O. (2007). Mixed and nonconforming finite element methods on a system of polygons. *Applied Numerical Mathematics*, *57*(2), 176–193. https://doi.org/10.1016/j.apnum.2006.02.005

Wang, C., Jiang, Y., Luan, H., & Sugimoto, S. (2020). Effect of shearing on hydraulic properties of rough-walled fractures under different boundary conditions. *Energy Science and Engineering*, *8*(3), 865–879. https://doi.org/10.1002/ese3.556

Warren, J. E., & Root, P. J. (1963). The Behavior of Naturally Fractured Reservoirs. *Society of Petroleum Engineers Journal*, *3*(03), 245–255. https://doi.org/10.2118/426-pa

Watanabe, N., Hirano, N., & Tsuchiya, N. (2009). Diversity of channeling flow in heterogeneous aperture distribution inferred from integrated experimental-numerical analysis on flow through shear fracture in granite. *Journal of Geophysical Research: Solid Earth*, *114*(4), 1–17. https://doi.org/10.1029/2008JB005959

Younes, A., Fahs, M., & Ahmed, S. (2009). Solving density driven flow problems with efficient spatial discretizations and higher-order time integration methods. *Advances in Water Resources*, *32*(3), 340–352. https://doi.org/10.1016/j.advwatres.2008.11.003

Zhang, K., & Woodbury, A. D. (2002). A Krylov finite element approach for multi-species contaminant transport in discretely fractured porous media. *Advances in Water Resources*, *25*(7), 705–721. https://doi.org/10.1016/S0309-1708(02)00084-2